Tropism illuminated: Lymphocyte-based pathways blazed by lethal morbillivirus through the host immune system

Veronika von Messling*, Dragana Milosevic, and Roberto Cattaneo†

Molecular Medicine Program and Virology and Gene Therapy Graduate Track, Mayo Clinic College of Medicine, Rochester, MN 55905

Edited by Charles Weissmann, University College London, London, United Kingdom, and approved August 13, 2004 (received for review May 25, 2004)

The immunosuppressive properties of morbilliviruses including measles and canine distemper virus (CDV) are well known, but the host cells supporting infection are poorly characterized. To identify these cells, a recombinant CDV expressing green fluorescent protein was produced by reverse genetics based on a wild-type strain lethal for ferrets. This recombinant virus fully retained virulence and blazed three lymphocyte-based pathways through the immune system of its host: first, it infected rapidly and massively circulating B and T cells; second, it took over and damaged secondary lymphatic organs including spleen, lymph nodes, and gut-associated and mucosal lymphoid tissues; third, it infected most thymocytes. In contrast, replication in epithelial cells was initially not detectable, but substantial before host death. Thus, CDV initially infects lymphocytes and massively replicates therein, thereby causing immunosuppression and preparing systemic invasion and host escape.

virus | measles | immunosuppression

In 1908, von Pirquet (1) observed that, in individuals with acute measles, tuberculin test responses are transiently depressed. Subsequent studies identified transiently lowered leukocyte counts and antibody titers, reduced *in vitro* lymphocyte proliferation activity, and polarization of the cellular immune response toward the Th2 pathway as immunosuppression landmarks (2–4). Little direct experimental evidence is available regarding the cell types supporting primary measles virus (MV) replication, or the quality and quantity of the immune cells infected during acute viral infections, but recently the signaling lymphocyte activating molecule (SLAM, CD150) was identified as an MV receptor (5, 6), suggesting a causal link between specific viral entry in lymphocytes and immunosuppression. Moreover, MV interactions with the ubiquitous regulator of complement activation membrane cofactor protein (MCP, CD46) (7–10) have been documented. Not only receptor choice but also postentry host cell control and immune evasion mechanisms determine MV tropism (11–13).

The lack of a small animal model has limited *in vivo* studies of MV pathogenesis. Only primates develop a measles-like disease (14–16); initial attempts to produce appropriately genetically modified mice have been only partially successful (17–19). Thus, other experimental paradigms have been sought (20), and recently a model of morbillivirus-induced pathogenesis was developed in ferrets, one of the natural canine distemper virus (CDV) hosts. CDV uses the same primary receptor (SLAM) as the other morbilliviruses (21), and, in small carnivores, it occupies the same ecological niche as MV in primates or rinderpest in ungulates. In ferrets, CDV infection causes a measles-like syndrome: disease signs include fever, whole body rash, drops in leukocyte numbers and lymphocyte proliferation activity, and respiratory and gastrointestinal symptoms (22). In ferrets, CDV is very virulent and causes animal death within 2–3 weeks, similar to infection of Bovidae with rinderpest (23). In dogs, CDV is approximately as virulent as MV in humans (24).

In view of these facts, we reasoned that CDV infection of ferrets may be an ideal model to gain insights in the cell types supporting morbillivirus replication and pathogenesis. Toward this end, we produced a recombinant CDV expressing a reporter gene that can be easily imaged. With this virus, we have been able to visually display lymphocytic involvement in the immunosuppressive process, the sequence of tissues infected, and the course of infection until death of the animal.

Materials and Methods

Generation of Enhanced GFP (eGFP)-Expressing 5804P Derivatives. An additional transcription unit (ATU) coding for the eGFP ORF was introduced at three different sites in the viral genome. The following three-step cloning strategy was used: (*i*) generation of three individual fragments coding for the region between the closest upstream located unique restriction site including the complete intergenic region followed by an *Asc*I site (fragment a), the eGFP ORF framed by *Asc*I and *Pac*I sites (fragment b), and a duplication of the intergenic region (fragment c, which begins with a *Pac*I site followed by the sequence of the downstream gene until the next unique restriction site); (*ii*) assembly of the three fragments into an intermediate plasmid by using *Asc*I and *Pac*I; (*iii*) introduction of the insert of the intermediate plasmid into the full-length 5804P plasmid by using the respective unique restriction sites. This strategy yielded pCDV/5804P-eGFP/uN, pCDV/5804P-eGFP/P, and pCDV/5804P-eGFP/H with the eGFP ATU.

All viruses were recovered by using the procedure described in ref. 22. The B cell-derived cell line B95a (25) was used as host, thus limiting replication in nonlymphoid cells that may affect virulence. These cells were transfected with plasmids expressing the three proteins of the CDV polymerase complex (N, P, and L) and a full-length CDV genomic plasmid by using Lipofectamine as detailed (26), and infected with a modified vaccine Ankara virus expressing the T7 RNA polymerase (27). After 3 days, the B95a cells were overlaid on VerodogSLAMtag cells that served as indicator: within 24–48 h, syncytia were detected and transferred back to B95a cells to obtain virus stocks.

Animal Experiments and Imaging. Animal experiments including the assays assessing the immune response and degree of immunosuppression were performed exactly as described in ref. 22; each ferret was inoculated intranasally with 10^4 infectious units. Macroscopic imaging was performed by using the MacroIllumi-

This paper was submitted directly (Track II) to the PNAS office.

Abbreviations: CDV, canine distemper virus; MV, measles virus; eGFP, enhanced GFP; MM, monocyte/macrophage; SLAM, signaling lymphocyte activating molecule; PBMC, peripheral blood mononuclear cell; d.p.i., days postinfection.

*Present address: Institut National de la Recherche Scientifique-Institut Armand-Frappier, Université du Québec, Laval, QC, Canada H7V 1B7.

†To whom correspondence should be addressed at: Molecular Medicine Program, Mayo Clinic, Guggenheim 1838, 200 First Street SW, Rochester, MN 55905. E-mail: cattaneo.roberto@mayo.edu.

www.pnas.org/cgi/doi/10.1073/pnas.0403597101

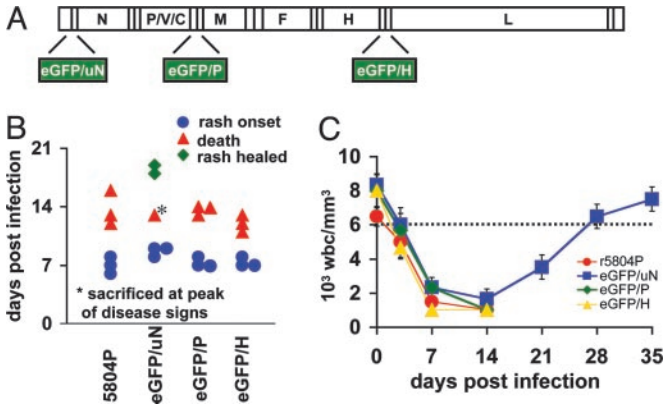

Fig. 1. Recombinant CDV expressing 5804P-eGFP/H retains wild-type virulence. (*A*) Different locations of the eGFP gene in the CDV genome. (*B*) Comparison of disease progression in animals infected with the parental or the eGFP-expressing viruses. Onset of rash is indicated by blue dots, time of death by red triangles, and healing of rash by green rhombus. Each pair of symbols represents one animal. (*C*) Leukocyte count of animals infected with the different viruses (same animals as in *B*). Blood samples were taken at the indicated time points. Error bars are included for each data point. The leukocyte concentration (6,000 cells per mm^3) below which animals are considered leukopenic is indicated by a dotted line. wbc, white blood cells.

nation Imaging System (Lightools, Encinitas, CA). Microscopic images of the different organs were obtained by transferring fresh organ cuts into a round glass dish (0.17-mm thickness; Bioptechs, Butler, PA), followed by visualization of eGFP expression by using an inverted fluorescent microscope (Nikon) for the lower magnifications (×4, ×10, and ×20), and an inverted confocal laser scanning microscope (Zeiss) for ×40 magnification.

Fluorescence-Activated Cell Sorter (FACS) Analysis and Immunohistochemistry. For FACS (Becton Dickinson) analysis, Ficoll gradient centrifugation-purified peripheral blood mononuclear cells (PBMCs), or single-cell suspensions obtained from thymus, spleen, or lymph node homogenates after hypotonic lysis of erythrocytes, were fixed overnight in 1% paraformaldehyde before incubation with Alexa 647-labeled monoclonal antibodies against CD3 (sc-20047, Santa Cruz Biotechnology), CD79α (DAKO), or CD14 (Veterinary Medical Research and Development, Pullman, WA), or a corresponding isotype control for 1 h. Alexa 647 and eGFP expression of each sample was assessed by using a FACScan instrument (Becton Dickinson).

For immunohistochemistry, formalin-fixed paraffin sections were deparaffinized, rehydrated, and incubated with a murine monoclonal antibody specific for the CDV nucleocapsid (N) protein (Veterinary Medical Research and Development, Pullman, WA), or a corresponding isotype control. The signal was amplified by using a biotinylated goat anti-mouse serum (DAKO), followed by incubation with peroxidase-labeled streptavidin (Amersham Pharmacia Biosciences). Peroxidase was visualized with 3-amino-9-ethylcarbazole as a substrate, yielding a red reaction product. Slides were counterstained with hematoxylin (Zymed).

Results

Introduction of an eGFP Reporter Gene into a Morbillivirus Genome Without Virulence Loss. We introduced the eGFP gene in three alternative positions in a plasmid containing the genomic sequence of the virulent strain 5804P (22): upstream of the N gene (5804P-eGFP/uN, virus A), between the P and M genes (5804P-eGFP/P, virus B), or between the H and L genes (5804P-eGFP/H, virus C) (Fig. 1*A*). Decreasing levels of reporter protein are produced by these three vectors (data not shown) due to the morbillivirus transcription gradient (28). Virus A was attenuated in ferrets, whereas viruses B and C retained wild-type virulence (Fig. 1*B*). All viruses caused severe leukopenia, but animals infected with virus A recovered (Fig. 1*C*, blue squares), whereas animals infected with viruses B or C died after ≈2 weeks as animals infected with 5804P (Fig. 1 *B* and *C*). In the virus B- or virus C-infected animals, body temperature, lymphocyte proliferation activity, and viremia had similar kinetics to those in 5804P control infections (22), whereas virus A infections had similar pathogenic consequences to those of infection with a partially attenuated strain (data not shown). Thus, an eGFP reporter gene was successfully introduced into a morbillivirus genome without inducing loss of virulence.

Sites of Preferential CDV Replication Include Lymph Nodes and Peyer's Patches. For all following experiments, we selected virus C and examined its spread by monitoring green light emission in infected animals that were killed at 7 (Fig. 2*A*) or 14 (Fig. 2*B*) days postinfection (d.p.i.). At 7 d.p.i. (rash appearance), whole-body examination revealed specific fluorescence in lymph nodes, and in Peyer's patches in the small intestine (Fig. 2*A Right*, LN and PP, respectively). At 14 d.p.i., sites of preferential virus replication continued to include lymph nodes and Peyer's patches, but eGFP signals were stronger than at 7 d.p.i. Fig. 2*E* shows a close-up of a small intestine section, illustrating the regular arrangement of carnivores Peyer's patches (29). To monitor the spread of infection in more detail, we dissected a segment of the small intestine at an earlier infection stage (4 d.p.i.) and analyzed it with a confocal microscope. Fig. 2*G* shows an infected Peyer's patch follicle: single infected cells are visible as well as larger infected structures, probably syncytia (one indicated with a white star). The three-dimensional localization of precisely confined infection centers within noninfected tissue is at best visualized by rotation of the confocal microscopy dataset (Movie 1, which is published as supporting information on the PNAS web site). At later time points, many more cells in a Peyer's patch were infected (data not shown).

Examination of the pharyngeal region after killing of a moribund animal revealed strong replication in the tonsils and infection of epithelial cells lining esophagus and trachea (Fig. 2*C*). In the spleen, white pulp areas were selectively infected (Fig. 2*D Left* and *Center*). By hematoxylin/eosin (H&E) staining (Fig. 2*F Left*), disruption of normal tissue architecture, acute inflammation, frequent small syncytia (white stars), and necrosis (black star) were observed. Secondary lymphoid follicles were poorly developed, but occasionally germinal centers with intact structures were detected within the white pulp (Fig. 2*F Right*). Thus, sites of preferential CDV replication include lymph nodes, Peyer's patches, and the spleen's white pulp.

Infection Spreads to Different Cell Types, Including Epithelial Cells. Infection was not limited to lymphatic cells, and, at killing, different tissues were emitting green light. Macroscopic examination of the skin in daylight or after fluorescence excitation 12 days after intranasal inoculation indicated that virus replication colocalized with the rash and involved the mucosal tissue in the palate (Fig. 2*H*, compare *Upper* and *Lower*). Analysis of lung tissue revealed confined areas of extensive replication (Fig. 2*I*). Rotation of the confocal microscopy dataset of Fig. 2*I* (Movie 2, which is published as supporting information on the PNAS web site) suggested that infection was confined to a single lobule and probably to its epithelial cells.

To verify which cell types sustain CDV replication in late infection stages, the distribution of the viral N protein was characterized by immunohistochemistry of bladder tissue. Transitional epithelial cells lining the luminal side of the emptied, contracted bladder were extensively infected by CDV, as visu-

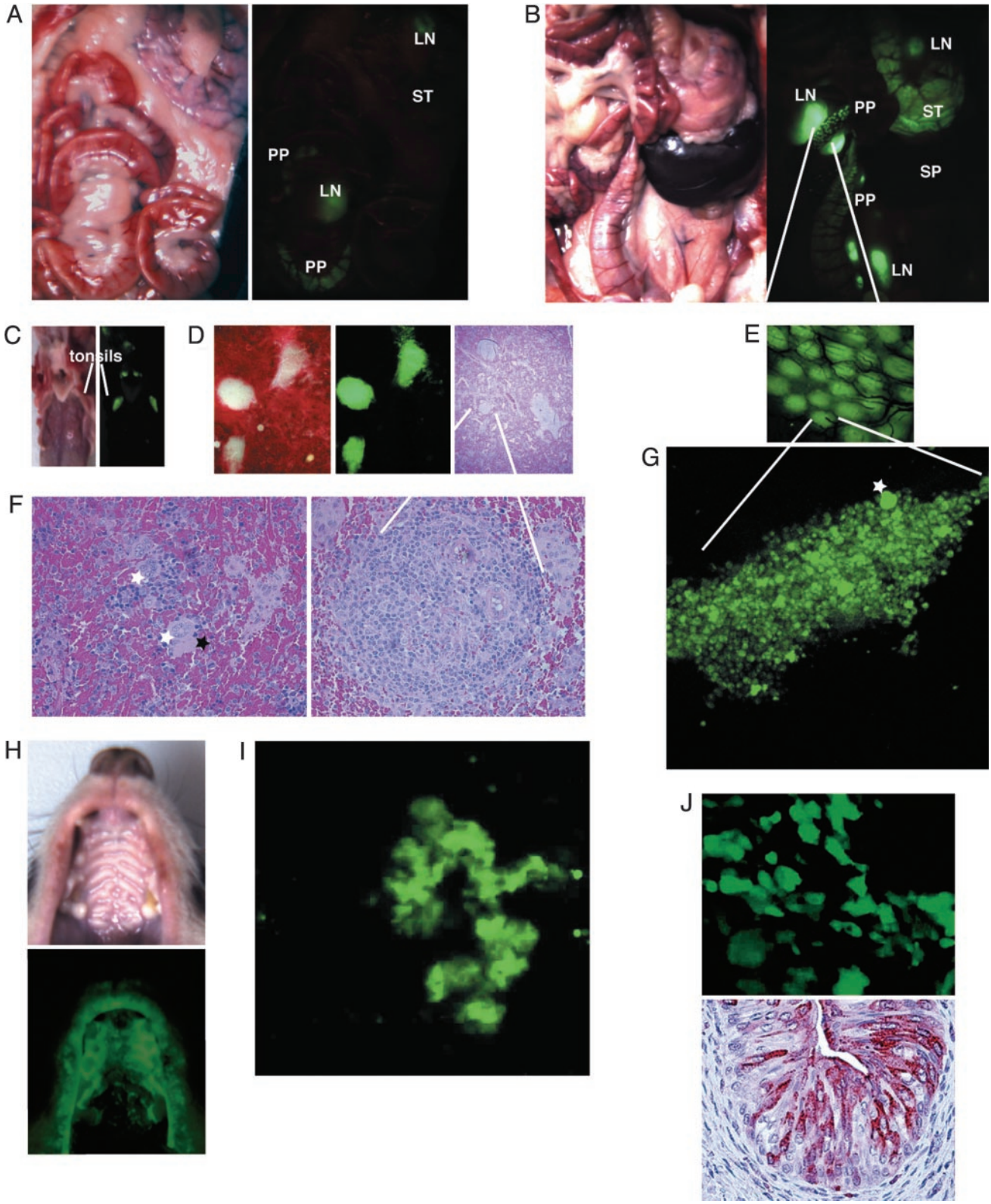

Fig. 2. CDV 5804P-eGFP/H replication is detected initially in lymphoid organs and then spreads to epithelial tissues. Daylight and fluorescent photos of the abdominal cavity of animals infected with 5804P-eGFP/H at 7 (*A*) or 14 (*B*) d.p.i. PP, Peyer's patches; LN, lymph node; ST, stomach; SP, spleen. (*C*) Daylight and fluorescent photos of the dissected throat at 7 d.p.i. (*D*) Daylight and fluorescent photographs of fresh spleen tissue (*Left* and *Center*) and corresponding hematoxylin/eosin (H&E)-stained paraffin-fixed section (*Right*). (*E*) Fluorescent photograph (intermediate magnification) of the Peyer's patches. (*F*) High-magnification H&E analysis of spleen regions with disrupted (*Left*) or normal (*Right*) morphology. White stars, syncytia; black star, necrotic region. (*G*) High-magnification image of a single Peyer's patch follicle. Star, larger infected structure (syncytium). (*H*) Daylight and fluorescent photos of an animal's oral cavity. (*I*) High magnification image of an infected lung lobulus. (*J*) Viral infection in the emptied, contracted bladder revealed by eGFP fluorescence (*Upper*) or nucleocapsid protein immunohistochemistry (*Lower*). (*Upper*) A surface view of flattened tissue. (*Lower*) A section through a tissue block.

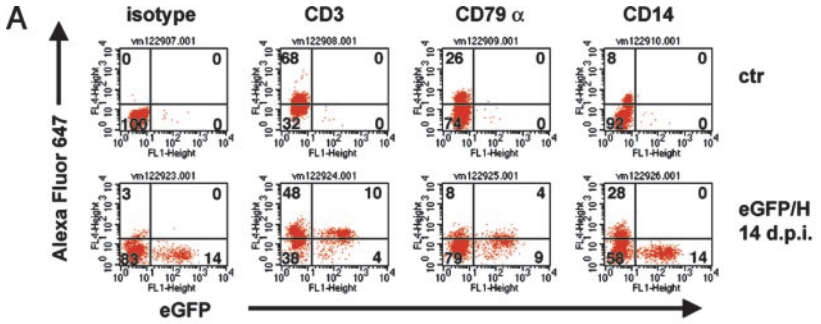

B

PBMC	CD3		CD79α		CD14	
	total	eGFP+ /%	total	eGFP+/%	total	eGFP
D0	61 (±4)	0	30 (±2)	0	11 (±3)	0
D7	35 (±5)	14 (±2) /40	14 (±2)	8 (±2) /57	49 (±3)	0
D14	58 (±1)	11 (±3) /19	14 (±1)	4 (±1) /29	30 (±1)	0

C

LN/SP/TY	CD3		CD79α		CD14	
	total	eGFP+	total	eGFP+	total	eGFP+
D0	54/65/89	0/ 0/ 0	45/32/ 9	0/ 0/ 0	0/ 2/ 0	0/ 0/ 0
D7	69/78/84	67/45/57	34/22/15	33/15/ 11	0/ 3/ 1	0/ 3/ 1
%eGFP+		97/58/68		97/68/ 73		
D14	54/79/88	50/44/81	49/18/14	31/12/ 14	0/ 3/ 0	0/ 3/ 0
%eGFP+		92/56/92		63/66/100		

Fig. 3. Time course and cell type specificity of CDV infections of PBMCs and lymphoid organs. (*A*) Fluorescence-activated cell sorter analysis of PBMCs isolated from an animal infected with 5804P-eGFP/H at 14 d.p.i. (*Lower*), and a noninfected control animal (*Upper*). Cells were stained with Alexa Fluor 647-labeled antibodies against cellular markers (*y* axis, see *Mateials and Methods*). eGFP expression was plotted on the *x* axis. (*B*) Percentages of CDV-infected T cells (CD3 positive), B cells (CD79α-positive), and MMs (CD14-positive). Groups of four animals were infected, and PBMCs were collected 0 (D0), 7 (D7), or 14 (D14) d.p.i. The mean values are indicated, with SD shown parenthetically. Total cells include eGFP-positive (eGFP+) cells. (*C*) CDV-infected cells in the lymph nodes (LN), spleen (SP), or thymus (TY) of animals killed 7 (D7) or 14 (D14) d.p.i., or a control animal (D0). In the lines labeled %eGFP+, the percentages of GFP-expressing (CDV-infected) cells within one cell type are indicated.

alized by specific red staining (Fig. 2*J Lower*). As expected, the red staining was limited to the cytoplasm, and the nuclei were excluded. GFP expression in fresh bladder tissue was also restricted to single cells as N protein expression in fixed tissue (Fig. 2*J Upper*), but, as expected, the nucleus was not excluded. Thus, in late infection stages, CDV replication can be monitored in different cell types, including epithelial cells in the bladder. In addition, we consistently recovered virus from ferret urine (unpublished data).

Massive Circulating Lymphocyte Infection Causes Lymphopenia. We then asked how extensive is PBMC infection and which cell types serve as CDV hosts. Only few ferret-specific antibodies are available and therefore pan-species antibodies directed against conserved epitopes of the CD3 T cell marker, the CD79α B cell marker, and the CD14 marker of the monocyte/macrophage (MM) lineage were used. In infected ferrets, the total number of PBMCs dropped to ≈20% of the standard within 7 d.p.i., that is, before rash appearance, and stayed low (Fig. 1*C*). At that time the relative number of lymphocytes decreased, whereas that of MMs increased (Fig. 3 *A* and *B*, compare CD3 and CD79α "total" columns with CD14 "total" columns). This event is due to the cytotoxic effect of CDV infection on lymphocytes: 7 d.p.i. ≈40% of the T and 60% of the B lymphocytes were infected, whereas no infected MMs were detected (Fig. 3*B*, line D7, compare $eGFP^+$/% data in CD3, CD79α, and CD14 cells, respectively). When examined *ex vivo*, eGFP-positive lymphocytes degenerated and died much faster than eGFP-negative cells from the same animal (data not shown). At 14 d.p.i., the percentage of infected T and B cells dropped to ≈20% and 30%, respectively, and their relative numbers recovered (Fig. 3*B*, line D14, $eGFP^+$/% data in CD3 and CD79α cells, respectively). Thus, circulating B and T lymphocytes are the main CDV infection targets, and their infection is extensive. This result is consistent with expression of SLAM, the primary cellular receptor for wild-type morbilliviruses, including CDV (21), on activated circulating T and B lymphocytes.

Massive Infection of B and T Lymphocytes in Lymph Nodes, Spleen, and Thymus. To examine the levels of CDV infection in lymphatic organs, two ferrets were killed 7 or 14 d.p.i., and their lymph nodes, spleen, and thymus were prepared. Extremely high percentages of eGFP-positive lymphocytes were monitored in lymph nodes and thymus (68–100%), and 56–68% spleen lymphocytes were infected (Fig. 3*C*, lines D7/%$eGFP^+$ and D14/%$eGFP^+$). The levels of infection of MM lineage cells in lymphatic organs were very low. Thus, lymphocyte infection in thymus and secondary lymphatic organs is not only rapid but also massive.

Discussion

Here, we present visual documentation of the course of a lethal animal virus infection in a natural host. Our analysis revealed an unexpectedly rapid and massive attack on host lymphocytes, resulting in immunosuppression. Three populations were affected. First, circulating B and T cells were infected. Second, lymphocytes residing in secondary lymphoid tissues were affected. As a consequence of infection, the architecture of the spleen and lymph nodes was partially destroyed; moreover, the observation that Peyer's patches and tonsils are heavily infected suggests that mucosal antibody response (IgA) that protects against pathogens entering from epithelial barriers is compro-

mised. Third, primary thymocytes were infected. Infection of lymphocytes in the primary lymphoid organs may be a decisive factor in pathogenesis, as it is for HIV type I (30). Thus, within 1 week, CDV completely compromised the immune system, while replicating extensively and disseminating in the organism.

Our analysis provided both a global and a detailed view of viral infection, macroscopically at the organ level and microscopically at the single-cell level, and enabled us to directly associate viral replication with specific disease signs, for example, the rash. Our observations suggest the following sequence of events in a morbillivirus infection. Viral particles infect lymphocytes located in lymphatic tissues of the oral cavity. The virus replicates rapidly and massively in these cells. Lymphocytes disseminate infection in the organism; in particular, epithelia are infiltrated by lymphocytes that occasionally may succumb to the infection load and locally release virus. Lung epithelium infection may be initiated from the basal side, consistent with the observation that MV preferentially transduces the basolateral surface of well-differentiated human airway epithelia (31). This sequence of events is different from previous morbillivirus infection models: based on limited evidence, it was assumed that the initial MV infection is established in the respiratory tract (2, 3). We detected CDV replication in the epithelial cells from the upper respiratory tract only at later infection stages.

May lymphocytes serve as the initial vehicle for the spread of other morbillivirus infections? The systematic analysis of tissues and organs of dogs infected with CDV and cows inoculated with rinderpest revealed that tonsils and pharyngeal and bronchial lymph nodes stained positive for viral antigen as early as 1 d.p.i. by aerosol whereas positive cells in the lung were detected between 3 and 6 d.p.i. (32, 33). Analogously, in the tracheal and bronchial epithelium of CDV-infected ferrets killed at days 2 or 4 after inoculation, GFP expression was not detectable (data not shown). In contrast, GFP expression was always clearly documented 4 d.p.i. and occasionally 2 d.p.i. in lymph nodes and Peyer's patches. Together, these findings suggest that, after intranasal inoculation, two animal morbilliviruses spread initially in the lymphoepithelial tissues of the tonsils and in lymphocytes resident in the upper respiratory tract mucosal lymphoid tissue.

How relevant is lymphocyte infection for measles? Infection of tissue lymphocytes during acute measles has been documented but not quantified (34–36). Up to 5% infected PBMCs were detected in one measles patient from whom blood was obtained 3 days after rash appearance, and much lower levels were detected in patients from whom blood was obtained a few days later (35). By analogy, we suspect that MV infection peaks at or before rash also in humans. Data about the types of MV-infected PBMCs are limited: in one study 1 in 125 to 1 in 2,500 MV-infected monocytes were detected (37), and fewer infected lymphocytes were detected. In contrast, many more infected lymphocytes than monocytes are detected in ferrets. Because MV occupies in primates the same ecological niche as CDV and rinderpest in small carnivores and ungulates, respectively, we suspect that it exploits lymphocytes as its primary host cells, and that the levels of MV replication in human lymphocytes need to be reevaluated.

What are the mechanisms of epithelial cell infection? Epithelial cells do not express SLAM, and alternative CDV receptors are not known. The ubiquitous protein human CD46 can act as an MV receptor in cultured cells and possibly also in humans infected with wild-type MV (38, 39), but CDV may not interact with CD46 (40). Morbilliviruses are highly cell-associated, but lymphocytes succumbing to the infection when patrolling epithelia may locally release high amounts of virus particles favoring cell entry through proteins that have lower affinity for the viral attachment protein than SLAM. Invasion of certain epithelia (lung and bladder) will elicit release of massive virus amounts before host death.

There have been many animal experiments with DNA and RNA viruses expressing reporter genes. Most of these studies have been done in rodents, in which it is not always possible to assert pathogenesis and compare virulence. Here, we have presented an example of a recombinant animal virus fully retaining virulence in a natural host while expressing a fluorescent reporter protein. The imaging technology used here may be generalized to other viruses, allowing unambiguous identification of cell types relevant for primary replication. This information is necessary to perfect antiviral drug assays. A relevant subject for future studies is HIV (41): it may be possible to visualize the host cells in the rectum or genital tract after experimental infection of macaques with an eGFP-expressing recombinant virus. Remarkably, the massive acute infection characterized here for a morbillivirus is reminiscent of the rapid production of large quantities of virus in lymph nodes of HIV patients, sometimes causing the nodes to swell (lymphoadenopathy). Engineering of a "brilliant" recombinant lentivirus fully retaining virulence should be possible, even if it may be less straightforward than that of a morbillivirus whose particles lack icosahedral symmetry and therefore have variable cargo volume (42) and tolerate well foreign gene insertion (43).

We thank C. Gorman, D. McKean, L. Pease, C. Springfeld, and R. Vile for reviewing the manuscript. This work was supported by National Institutes of Health Grant R01 CA90636 and grants from the Siebens and Mayo Foundations.

1. von Pirquet, C. (1908) *Dtsch. Med. Wochenschr.* **30,** 1297–1300.
2. Borrow, P. & Oldstone, M. B. (1995) *Curr. Top. Microbiol. Immunol.* **191,** 85–100.
3. Griffin, D. E. (2001) in *Fields Virology*, eds. Knipe, D. M. & Howley, P. M. (Lippincott Williams & Wilkins, Philadelphia), Vol. 1, pp. 1401–1441.
4. Moss, W. J., Ryon, J. J., Monze, M. & Griffin, D. E. (2002) *J. Infect. Dis.* **186,** 879–887.
5. Tatsuo, H., Ono, N., Tanaka, K. & Yanagi, Y. (2000) *Nature* **406,** 893–897.
6. Hsu, E. C., Iorio, C., Sarangi, F., Khine, A. A. & Richardson, C. D. (2001) *Virology* **279,** 9–21.
7. Cattaneo, R. (2004) *J. Virol.* **78,** 4385–4388.
8. Karp, C. L., Wysocka, M., Wahl, L. M., Ahearn, J. M., Cuomo, P. J., Sherry, B., Trinchieri, G. & Griffin, D. E. (1996) *Science* **273,** 228–231.
9. Naniche, D., Varior-Krishnan, G., Cervoni, F., Wild, T. F., Rossi, B., Rabourdin-Combe, C. & Gerlier, D. (1993) *J. Virol.* **67,** 6025–6032.
10. Dorig, R. E., Marcil, A., Chopra, A. & Richardson, C. D. (1993) *Cell* **75,** 295–305.
11. Avota, E., Avots, A., Niewiesk, S., Kane, L. P., Bommhardt, U., ter Meulen, V. & Schneider-Schaulies, S. (2001) *Nat. Med.* **7,** 725–731.
12. Marie, J. C., Kehren, J., Trescol-Biemont, M. C., Evlashev, A., Valentin, H., Walzer, T., Tedone, R., Loveland, B., Nicolas, J. F., Rabourdin-Combe, C. & Horvat, B. (2001) *Immunity* **14,** 69–79.
13. Palosaari, H., Parisien, J. P., Rodriguez, J. J., Ulane, C. M. & Horvath, C. M. (2003) *J. Virol.* **77,** 7635–7644.
14. Zhu, Y. D., Heath, J., Collins, J., Greene, T., Antipa, L., Rota, P., Bellini, W. & McChesney, M. (1997) *Virology* **233,** 85–92.
15. Auwaerter, P. G., Rota, P. A., Elkins, W. R., Adams, R. J., DeLozier, T., Shi, Y., Bellini, W. J., Murphy, B. R. & Griffin, D. E. (1999) *J. Infect. Dis.* **180,** 950–958.
16. Stittelaar, K., Wyatt, L., de Swart, R., Vos, H., Groen, J., van Amerongen, G., van Binnendijk, R., Rozenblatt, S., Moss, B. & Osterhaus, A. (2000) *J. Virol.* **74,** 4236–4243.
17. Roscic-Mrkic, B., Schwendener, R. A., Odermatt, B., Zuniga, A., Pavlovic, J., Billeter, M. A. & Cattaneo, R. (2001) *J. Virol.* **75,** 3343–3351.
18. Slifka, M. K., Homann, D., Tishon, A., Pagarigan, R. & Oldstone, M. B. (2003) *J. Clin. Invest.* **111,** 805–810.
19. Hahm, B., Arbour, N., Naniche, D., Homann, D., Manchester, M. & Oldstone, M. B. (2003) *J. Virol.* **77,** 3505–3515.
20. Niewiesk, S. (1999) *Immunol. Lett.* **65,** 47–50.
21. Tatsuo, H., Ono, N. & Yanagi, Y. (2001) *J. Virol.* **75,** 5842–5850.
22. von Messling, V., Springfeld, C., Devaux, P. & Cattaneo, R. (2003) *J. Virol.* **77,** 12579–12591.
23. Barrett, T. & Rossiter, P. B. (1999) *Adv. Virus Res.* **53,** 89–110.

24. Appel, M. J., Shek, W. R. & Summers, B. A. (1982) *Infect. Immun.* **37,** 592–600.
25. Kobune, F., Sakata, H. & Sugiura, A. (1990) *J. Virol.* **64,** 700–705.
26. von Messling, V., Zimmer, G., Herrler, G., Haas, L. & Cattaneo, R. (2001) *J. Virol.* **75,** 6418–6427.
27. Sutter, G., Ohlmann, M. & Erfle, V. (1995) *FEBS Letter* **371,** 9–12.
28. Cattaneo, R., Rebmann, G., Schmid, A., Baczko, K., ter Meulen, V. & Billeter, M. A. (1987) *EMBO J.* **6,** 681–688.
29. Bacha, W. J., Jr., & Bacha, L. M. (2000) in *Color Atlas of Veterinary Histology*, ed. Balado, D. (Lippincott Williams & Wilkins, Philadelphia), pp. 69–84.
30. Brooks, D. G., Kitchen, S. G., Kitchen, C. M., Scripture-Adams, D. D. & Zack, J. A. (2001) *Nat. Med.* **7,** 459–464.
31. Sinn, P. L., Williams, G., Vongpunsawad, S., Cattaneo, R. & McCray, P. B., Jr. (2002) *J. Virol.* **76,** 2403–2409.
32. Appel, M. J. (1969) *Am. J. Vet. Res.* **30,** 1167–1182.
33. Plowright, W. (1964) *J. Hyg. (London)* **62,** 257–281.
34. Moench, T. R., Griffin, D. E., Obriecht, C. R., Vaisberg, A. J. & Johnson, R. T. (1988) *J. Infect. Dis.* **158,** 433–442.
35. Forthal, D. N., Aarnaes, S., Blanding, J., de la Maza, L. & Tilles, J. G. (1992) *J. Infect. Dis.* **166,** 421–424.
36. Sakaguchi, M., Yoshikawa, Y., Yamanouchi, K., Sata, T., Nagashima, K. & Takeda, K. (1986) *Microbiol. Immunol.* **30,** 1067–1073.
37. Esolen, L. M., Ward, B. J., Moench, T. R. & Griffin, D. E. (1993) *J. Infect. Dis.* **168,** 47–52.
38. Manchester, M., Eto, D. S., Valsamakis, A., Liton, P. B., Fernandez-Munoz, R., Rota, P. A., Bellini, W. J., Forthal, D. N. & Oldstone, M. B. (2000) *J. Virol.* **74,** 3967–3974.
39. Schneider, U., von Messling, V., Devaux, P. & Cattaneo, R. (2002) *J. Virol.* **76,** 7460–7467.
40. Galbraith, S. E., Tiwari, A., Baron, M. D., Lund, B. T., Barrett, T. & Cosby, S. L. (1998) *J. Virol.* **72,** 10292–10297.
41. Oldstone, M. B. (1996) *Proc. Natl. Acad. Sci. USA* **93,** 12756–12758.
42. Rager, M., Vongpunsawad, S., Duprex, W. P. & Cattaneo, R. (2002) *EMBO J.* **21,** 2364–2372.
43. Skiadopoulos, M. H., Surman, S. R., Riggs, J. M., Orvell, C., Collins, P. L. & Murphy, B. R. (2002) *Virology* **297,** 136–152.